Mixed-Precision Arrangement via CRB for DOA Estimation Using SLA

Xinnan Zhang, Yuanbo Cheng, Xiaolei Shang and Jun Liu
Department of Electronic Engineering and Information Science
University of Science and Technology of China
Hefei, Anhui, China
Email: {zhangxinnan,cyb967,xlshang}@mail.ustc.edu.cn, junliu@ustc.edu.cn

***Abstract*—We consider a mixed analog-to-digital converter (ADC) based architecture for the direction of arrival (DOA) estimation under sparse linear arrays (SLAs) with arbitrary structure. Given the fixed number of ADCs, the arrangement of high-precision and one-bit ADCs in SLA is analyzed using Cramér-Rao bound (CRB). To obtain the optimal mixed-precision arrangement, we simplify the problem into a 0-1 integer quadratic programming and efficiently solve it by using the alternating direction method of multipliers (ADMM) algorithm. Simulation results validate the effectiveness of our approach. Furthermore, SLAs, such as the nested and co-prime array, can achieve a lower CRB with the optimal mixed-precision arrangement.**

***Index Terms*—Cramér-Rao bound (CRB), direction of arrival (DOA), mixed-ADC based architecture, mixed-precision arrangement, sparse linear array (SLA).**

I. Introduction

The estimation of direction of arrival (DOA) is a crucial problem in the field of array signal processing, with numerous applications in automotive radar, sonar, and unmanned aerial vehicles [1–3]. DOA estimation using uniform linear arrays (ULAs) has received considerable attention in recent decades. However, the number of identifiable sources is limit by the number of sensors [4, 5]. Due to specific geometries, sparse linear array (SLA), such as minimum redundancy arrays [6], co-prime arrays [7] and nested arrays [8], can identify more sources and achieve higher angular resolution than the ULA. With SLAs, numerous algorithms based on data, sampled by high-precision analog-to-digital converters (ADCs), have been proposed to address the problem of DOA estimation. However, as the quantization bit and sampling rate increase, the power consumption and hardware cost of ADC increase exponentially [9], making it impractical to use large scale high-precision ADC systems, e.g., receive antennas in high-level autonomous driving.

One-bit ADC has recently emerged as a promising technique [10–13] for mitigating the aforementioned ADC problems. However, using a pure one-bit ADC system can lead to some problems such as a large rate loss in high signal-to-noise ratio (SNR) regime [14] and dynamic range problem (i.e., a strong target can mask a weak target [9]). To address these issues, a mixed-ADC based architecture has been proposed in [15], where most receive antenna outputs are sampled by one-bit ADCs and a few by high-resolution ADCs. Previous studies have investigated the approximate DOA performance loss [16] and Cramér-Rao bound (CRB) in phase-modulated continuous-wave multiple-input multiple-output radar [17] with a mixed-ADC architecture. However, they did not exploit the full potential of the mixed-ADC architecture, as they used high-precision ADCs on one side and one-bit ADCs on the other side. Although the arrangement of high-precision and one-bit ADCs in ULA has been analyzed in [18] based on the property of symmetry, it still remains a problem for SLAs with arbitrary structures.

Using CRB, this work investigates the mixed-precision arrangement problem in SLAs with arbitrary structure under a mixed-ADC based architecture. We first derive the asymptotic CRB of the DOA in SLAs, and convert the problem into a simplified 0-1 integer quadratic programming problem. We employ the alternating direction method of multipliers (ADMM) algorithm to efficiently solve it. Numerical results demonstrate that the optimal mixed-precision arrangement can achieve better performance.

Notation: We denote vectors and matrices by bold lowercase and uppercase letters, respectively. $(\cdot)^T$ and $(\cdot)^H$ represent the transpose and the conjugate transpose, respectively. $\mathbf{I}_N$ denotes an $N \times N$ identity matrix and $\mathbf{1}_N = [1, \ldots, 1]^T \in \mathbb{R}^{N\times 1}$. $\otimes$, $\odot$ and $\circ$ denote the Kronecker, Khatri–Rao and Hadamard matrix products, respectively. $\|\cdot\|$ denotes the ℓ_2 norm. $\mathrm{vec}(\cdot)$ refers to the column-wise vectorization operation and $\mathrm{diag}(\mathbf{d})$ denotes a diagonal matrix with diagonal entries formed from $\mathbf{d}$. $\mathbf{A}_{\mathrm{R}} \triangleq \Re\{\mathbf{A}\}$ and $\mathbf{A}_{\mathrm{I}} \triangleq \Im\{\mathbf{A}\}$, where $\Re\{\cdot\}$ and $\Im\{\cdot\}$ denote the real and imaginary parts, respectively. $\mathrm{sign}(\cdot)$ is the sign function applied element-wise to vector or matrix. Finally, $j \triangleq \sqrt{-1}$.

II. Signal Model

We consider a SLA with M elements located at position $\{d_1\frac{\lambda}{2}, d_1\frac{\lambda}{2}, \ldots, d_M\frac{\lambda}{2}\}$ with $d_i \in \mathbb{D}$, where $\mathbb{D}$ is a set of integers with cardinality $|\mathbb{D}| = M$ and λ is the wavelength of

This work was supported in part by the National Natural Science Foundation of China under Contract 62271461, the Youth Innovation Promotion Association CAS (CX2100060053), and the Anhui Provincial Natural Science Foundation under Grant 2208085J17.

the signal. It is assumed that K narrowband far-field signals impinge on the array from different directions $\{\theta_1, \ldots, \theta_K\}$. After sampling and quantization, the array output can be stacked over the whole N snapshots as

$$\mathbf{X} = \mathbf{AS} + \mathbf{E}, \tag{1}$$

where $\mathbf{X} = [\mathbf{x}(1), \mathbf{x}(2), \ldots, \mathbf{x}(N)] \in \mathbb{C}^{M\times N}$ is the received signal matrix, $\mathbf{A} = [\mathbf{a}(\theta_1), \cdots, \mathbf{a}(\theta_K)] \in \mathbb{C}^{M\times K}$ represents the array steering matrix with

$$\mathbf{a}(\theta_k) = \left[e^{j\pi d_1 \sin\theta_k}, e^{j\pi d_2 \sin\theta_k}, \ldots, e^{j\pi d_M \sin\theta_k}\right]^T, \tag{2}$$

denoting the steering vector of the the kth source, $\mathbf{S} = [\mathbf{s}(1), \mathbf{s}(2), \ldots, \mathbf{s}(N)] \in \mathbb{C}^{K\times N}$ denotes the source signal matrix, and $\mathbf{E} = [\mathbf{e}(1), \mathbf{e}(2), \ldots, \mathbf{e}(N)] \in \mathbb{C}^{M\times N}$ is the noise sequence. The noise has the zero-mean circularly symmetric complex-valued white Gaussian distribution with independent and identically distributed (i.i.d.) known variance σ^2. The source signal matrix $\mathbf{S}$ is assumed to be deterministic but unknown, which is referred to as the conditional or deterministic model [5].

When one-bit ADC is employed with time-varying threshold for quantization, the array output is modified as

$$\mathbf{Z} = \mathcal{Q}(\mathbf{X} - \mathbf{H}), \tag{3}$$

where $\mathbf{H} \in \mathbb{C}^{M\times N}$ represents the known threshold and $\mathcal{Q}(\cdot) = \mathrm{sign}(\Re\{\cdot\}) + j\mathrm{sign}(\Im\{\cdot\})$ denotes the complex one-bit quantization operator.

We consider a mixed-ADC based architecture equipped with M_0 high-resolution ADCs and M_1 one-bit ADCs, where $M_0 + M_1 = M$. More generally, we define a high-precision ADC indicator vector $\boldsymbol{\delta} = [\delta_1, \ldots, \delta_M]^T$ with $\delta_i \in \{0, 1\}$, which means that the ith antenna is equipped with high-precision ADC when $\delta_i = 1$ or one-bit ADC when $\delta_i = 0$. So the mixed output can be represented as

$$\mathbf{Y} = \mathbf{Z} \circ (\bar{\boldsymbol{\delta}} \otimes \mathbf{1}_N^T) + \mathbf{X} \circ (\boldsymbol{\delta} \otimes \mathbf{1}_N^T), \tag{4}$$

where $\bar{\boldsymbol{\delta}} = \mathbf{1}_M - \boldsymbol{\delta}$ is the indicator for one-bit ADC.

Nest array and co-prime array are two popular sparse arrays. The nested array is composed of two ULAs which have different inter-element spacings. Specifically, a nested array with $N_1 + N_2$ sensors has the following sensor locations:

$$\mathbb{D}_{\text{nested}} = \{1, \ldots, N_1, (N_1+1), \ldots N_2(N_1+1)\}, \tag{5}$$

and the sensor locations for co-prime with $N_1 + 2N_2 - 1$ are given by

$$\mathbb{D}_{\text{co-prime}} = \{0, N_2, \ldots, (N_1-1)N_2, N_1, \ldots, (2N_2-1)N_1\}. \tag{6}$$

III. CRB OF THE DOA FOR MIXED DATA

Let $\boldsymbol{\varphi}$ collect all the real-valued unknown signal parameters, i.e., $\boldsymbol{\varphi} = \left[\boldsymbol{\theta}^T,\ \mathbf{s}_{\mathrm{R}}^T,\ \mathbf{s}_{\mathrm{I}}^T\right]^T \in \mathbb{R}^{(K+2KN)\times 1}$, where $\mathbf{s} = \mathrm{vec}(\mathbf{S})$.

In [18], the Fisher information matrix (FIM) for mixed data is given by

$$\mathbf{F}_m(\boldsymbol{\varphi}) = \frac{2}{\sigma^2}\Re\left\{\mathbf{U}_0\mathbf{U}_0^H\right\} + \frac{1}{\pi\sigma^2}\left(\mathbf{U}_{1,\mathrm{R}}\boldsymbol{\Lambda}_{\mathrm{R}}\mathbf{U}_{1,\mathrm{R}}^T + \mathbf{U}_{1,\mathrm{I}}\boldsymbol{\Lambda}_{\mathrm{I}}\mathbf{U}_{1,\mathrm{I}}^T\right). \tag{7}$$

Here, $\mathbf{U}_0 = \mathbf{U}\mathrm{diag}\left(\mathbf{1}_N \otimes \boldsymbol{\delta}\right)$ and $\mathbf{U}_1 = \mathbf{U}\mathrm{diag}\left(\mathbf{1}_N \otimes \bar{\boldsymbol{\delta}}\right)$ denote the derivatives of the high-precision and one-bit data with respect to $\boldsymbol{\varphi}$ respectively, where

$$\mathbf{U} = [\boldsymbol{\Delta},\quad \mathbf{G},\quad j\mathbf{G}]^H, \tag{8}$$

$$\boldsymbol{\Delta} = \mathbf{S}^T \odot \dot{\mathbf{A}},\quad \mathbf{G} = \mathbf{I}_N \otimes \mathbf{A}, \tag{9}$$

$$\dot{\mathbf{A}} = \left[\frac{\partial \mathbf{a}(\theta_1)}{\partial\theta_1}, \ldots, \frac{\partial \mathbf{a}(\theta_K)}{\partial\theta_K}\right]. \tag{10}$$

Additionally, $\boldsymbol{\Lambda} = \mathrm{diag}([\lambda_1, \ldots, \lambda_{MN}])$ where the diagonal element λ_k is given by

$$\lambda_k = B\left(\frac{\Re(\zeta_k)}{\sigma/\sqrt{2}}\right) + jB\left(\frac{\Im(\zeta_k)}{\sigma/\sqrt{2}}\right), \tag{11}$$

in which ζ_k is the kth element in $\boldsymbol{\zeta} = \mathrm{vec}(\mathbf{AS} - \mathbf{H}) \in \mathbb{C}^{MN\times 1}$ and the function $B(\cdot)$ is defined by

$$B(x) = \left[\frac{1}{\Phi(x)} + \frac{1}{\Phi(-x)}\right]e^{-x^2} \tag{12}$$

with $\Phi(x) = \int_{-\infty}^{x}\frac{1}{\sqrt{2\pi}}e^{-\frac{t^2}{2}}dt$ being the cumulative distribution function of the normal standard distribution.

Since the FIM of mixed data reaches its upper bound when $\mathbf{H} = \mathbf{AS}$ [19], we consider the simplified CRB that can be approximately achieved in a low SNR scene. So the asymptotic CRB of the DOA [18] can be given as

$$\mathrm{CRB}(\boldsymbol{\theta}) = \frac{\sigma^2}{2N}\Re\left\{\left(\dot{\mathbf{A}}^H\boldsymbol{\Omega}\dot{\mathbf{A}}\right) \circ \hat{\mathbf{P}}^T\right\}^{-1}, \tag{13}$$

where

$$\hat{\mathbf{P}} = \frac{1}{N}\sum_{t=1}^{N}\mathbf{s}(t)\mathbf{s}^H(t), \tag{14}$$

$$\boldsymbol{\Omega} = \boldsymbol{\Sigma}_0 - \boldsymbol{\Sigma}_0\mathbf{A}(\mathbf{A}^H\boldsymbol{\Sigma}_0\mathbf{A})^{-1}\mathbf{A}^H\boldsymbol{\Sigma}_0, \tag{15}$$

$$\boldsymbol{\Sigma}_0 = \left(1 - \frac{2}{\pi}\right)\mathrm{diag}(\boldsymbol{\delta}) + \frac{2}{\pi}\mathbf{I}_M. \tag{16}$$

Considering that the estimated power $\hat{\mathbf{P}}$ can be replaced by the true power $\mathbf{P}$ for sufficiently large N, the asymptotic CRB of the DOA is given by

$$\mathrm{CRB}(\boldsymbol{\theta}) = \frac{\sigma^2}{2N}\Re\left\{\left(\dot{\mathbf{A}}^H\boldsymbol{\Omega}\dot{\mathbf{A}}\right) \circ \mathbf{P}^T\right\}^{-1}. \tag{17}$$

A. CRB for K = 1

When a single target is considered, the asymptotic CRB of the DOA can be expressed as

$$\mathrm{CRB}(\theta) = \frac{M_0 + \frac{2}{\pi}M_1}{2\pi^2 S}\frac{1}{\mathrm{SNR}\cos^2\theta}, \tag{18}$$

where SNR $= p/\sigma^2$ and

$$S = \sum_{i=1}^{M} g_i d_i^2 \sum_{i=1}^{M} g_i - \left(\sum_{i=1}^{M} g_i d_i \right)^2, \tag{19}$$

in which $g_i \in \{1, \frac{2}{\pi}\}$ and $\sum_{i=1}^{M} g_i = M_0 + \frac{2}{\pi} M_1$.

B. Mixed-precision arrangement problem in SLA

It is found that the asymptotic CRB of the DOA is related to the arrangement of one-bit and high-precision ADCs. However, identifying the optimal mixed-precision arrangement is a combinatorial optimization problem which is recognized to be NP-hard.

Since the parameters of target and array are fixed, the asymptotic CRB is only concerned with S. By using Lagrange's identity, we can formulate the problem as

$$\begin{aligned} \max_{\{g_i\}_{i=1,2\cdots,M}} \quad & S = \sum_{i=1}^{M} \sum_{j>i} g_i g_j (d_j - d_i)^2 \\ \text{s.t.} \quad & g_i \in \{1, \frac{2}{\pi}\}, \quad i = 1, 2, \ldots, M, \\ & \sum_{i=1}^{M} g_i = M_0 + \frac{2}{\pi} M_1. \end{aligned} \tag{20}$$

By vectorizing the parameters and introducing a new variable $z_i \in \{0, 1\}$ such that $g_i = (1 - \frac{2}{\pi}) z_i + \frac{2}{\pi}$, the optimization objective can be rewritten as

$$\begin{aligned} S &= \frac{1}{2} \left(\left(1 - \frac{2}{\pi}\right) \mathbf{z} + \frac{2}{\pi} \mathbf{1}_M \right)^T \mathbf{D} \left(\left(1 - \frac{2}{\pi}\right) \mathbf{z} + \frac{2}{\pi} \mathbf{1}_M \right) \\ &= \frac{1}{2} \left(1 - \frac{2}{\pi}\right)^2 (\mathbf{z^T D z} + \mathbf{b}^T \mathbf{z}) + \frac{4}{\pi^2} \mathbf{1}_M^T \mathbf{D} \mathbf{1}_M \end{aligned} \tag{21}$$

where $\mathbf{z} = [z_1, z_2, \ldots, z_M]^T$, $\mathbf{D}$ is a matrix with $\mathbf{D}_{ij} = (d_i - d_j)^2$ and $\mathbf{b} = \frac{4}{\pi - 2} \mathbf{D} \mathbf{1}_M$. Thus, the mixed-precision arrangement problem can be reformulated as

$$\begin{aligned} \min_{\mathbf{z}} \quad & -\mathbf{z}^T \mathbf{D} \mathbf{z} - \mathbf{b}^T \mathbf{z} \\ \text{s.t.} \quad & \mathbf{z} \in \{0, 1\}^M, \\ & \mathbf{1}_M^T \mathbf{z} = M_0. \end{aligned} \tag{22}$$

IV. Optimization

The optimization problem (22) is a challenging 0-1 integer programming problem. Note that the binary constraint can be transformed to continuous constraint as follows [20]:

$$\mathbf{z} \in \{0, 1\}^M \Leftrightarrow \mathbf{z} \in S_b \cap \mathbf{z} \in S_p \tag{23}$$

where $S_b = [0, 1]^M$ denotes a box constraint, and $S_p = \left\{ \mathbf{z} : \left\| \mathbf{z} - \frac{1}{2} \mathbf{1}_M \right\|_2^2 = \frac{M}{4} \right\}$ indicates a ℓ_2-sphere constraint. With these constraints, we reformulated the problem (22) as

$$\begin{aligned} \min_{\mathbf{z}} \quad & -\mathbf{z}^T \mathbf{D} \mathbf{z} - \mathbf{b}^T \mathbf{z} \\ \text{s.t.} \quad & \mathbf{1}_M^T \mathbf{z} = M_0, \quad \mathbf{z} = \mathbf{z}_1, \quad \mathbf{z} = \mathbf{z}_2, \\ & \mathbf{z}_1 \in S_b, \quad \mathbf{z}_2 \in S_p, \end{aligned} \tag{24}$$

where $\mathbf{z}_1$ and $\mathbf{z}_2$ are two additional variables to decompose the box and the ℓ_2-sphere constraints on $\mathbf{z}$. Since the problem is non-convex, we use the ADMM to solve it.

Specifically, the augmented Lagrangian function of (24) is given by

$$\begin{aligned} &\mathcal{L}(\mathbf{z}, \mathbf{z}_1, \mathbf{z}_2, \boldsymbol{\eta}_1, \boldsymbol{\eta}_2, \eta_3) = -\mathbf{z}^T \mathbf{D} \mathbf{z} - \mathbf{b}^T \mathbf{z} + h_1(\mathbf{z}_1) + h_2(\mathbf{z}_2) \\ &+ \boldsymbol{\eta}_1^T (\mathbf{z} - \mathbf{z}_1) + \boldsymbol{\eta}_2^T (\mathbf{z} - \mathbf{z}_2) + \eta_3 (\mathbf{1}_M^T \mathbf{z} - M_0) \\ &+ \frac{\rho_1}{2} \|\mathbf{z} - \mathbf{z}_1\|_2^2 + \frac{\rho_2}{2} \|\mathbf{z} - \mathbf{z}_2\|_2^2 + \frac{\rho_3}{2} \|\mathbf{1}_M^T \mathbf{z} - M_0\|_2^2, \end{aligned} \tag{25}$$

where $\boldsymbol{\eta_1} \in \mathbb{R}^M$, $\boldsymbol{\eta_2} \in \mathbb{R}^M$, $\eta_3 \in \mathbb{R}$ are dual variables and (ρ_1, ρ_2, ρ_3) are positive penalty parameters. The function $h_1(\mathbf{z}_1) = \mathbb{I}_{\{\mathbf{z}_1 \in S_b\}}$ and $h_2(\mathbf{z}_2) = \mathbb{I}_{\{\mathbf{z}_2 \in S_p\}}$ are indicator function for sets S_b and S_p respectively, where

$$\mathbb{I}_a = \begin{cases} 0 & \text{when a is true} \\ +\infty & \text{when a is false} \end{cases} \tag{26}$$

Following the conventional ADMM, we update the primal and dual variables iteratively. Given the parameter estimates at iteration t, we obtain the updates as described below.

A. Update $\mathbf{z}^{t+1}$

When the other variables are fixed, the Lagrangian function with respect to $\mathbf{z}$ is convex. By setting the gradient to zero, $\mathbf{z}^{t+1}$ can be obtained directly as the solution to the following positive-definite linear system:

$$\begin{aligned} &(-2\mathbf{D} + (\rho_1 + \rho_2)\mathbf{I} + \rho_3 \mathbf{1}_M \mathbf{1}_M^T) \mathbf{z}^{t+1} = \\ &\quad \rho_1 \mathbf{z}_1^t + \rho_2 \mathbf{z}_2^t + M_0 \rho_3 \mathbf{1}_M + \mathbf{b} - \boldsymbol{\eta}_1^t - \boldsymbol{\eta}_2^t - \eta_3^t \mathbf{1}_M, \end{aligned} \tag{27}$$

Remark 1. *It is worth noting that, for $\mathbf{z} \in \{0, 1\}^M$, we have $\mathbf{z}^T \mathbf{z} = \mathbf{1}_M^T \mathbf{z}$. Furthermore, since $-\mathbf{z}^T \mathbf{D} \mathbf{z} = \mathbf{z}^T (\alpha \mathbf{I} - \mathbf{D}) \mathbf{z} - \alpha \mathbf{1}_M^T \mathbf{z}$ for any α, we can assume that $-\mathbf{D}$ is positive semi-definite. Thus, (27) can be efficiently solved by using the preconditioned conjugate gradient method.*

B. Update ($\mathbf{z}_1^{t+1}$, $\mathbf{z}_2^{t+1}$)

The vectors $\mathbf{z}_1$ and $\mathbf{z}_2$ are updated via the following optimization problems:

$$\mathbf{z}_1 = \arg\min_{\mathbf{z_1}} \quad h_1(\mathbf{z_1}) + \frac{\rho_1}{2} \|\mathbf{z} - \mathbf{z}_1\|_2^2 + \boldsymbol{\eta}_1^T (\mathbf{z} - \mathbf{z}_1), \tag{28}$$

$$\mathbf{z}_2 = \arg\min_{\mathbf{z_2}} \quad h_2(\mathbf{z_2}) + \frac{\rho_2}{2} \|\mathbf{z} - \mathbf{z}_2\|_2^2 + \boldsymbol{\eta}_2^T (\mathbf{z} - \mathbf{z}_2). \tag{29}$$

The solutions can be obtained by projecting the vector $\mathbf{z}$ onto the box constraint S_b and ℓ_2-sphere constraint S_p, respectively, which gives that

$$\mathbf{z}_1^{t+1} = \mathbf{P}_{S_b} \left(\mathbf{z}^{t+1} + \frac{1}{\rho_1} \boldsymbol{\eta}_1^t \right), \tag{30}$$

$$\mathbf{z}_2^{t+1} = \mathbf{P}_{S_p} \left(\mathbf{z}^{t+1} + \frac{1}{\rho_2} \boldsymbol{\eta}_2^t \right), \tag{31}$$

where $\mathbf{P}_{S_b}(\mathbf{x}) = \min(\mathbf{1}_M, \max(\mathbf{0}_M, \mathbf{x}))$ and $\mathbf{P}_{S_p}(\mathbf{x}) = \frac{\sqrt{M}}{2} \frac{\mathbf{x} - \frac{1}{2}\mathbf{1}_M}{\|\mathbf{x} - \frac{1}{2}\mathbf{1}_M\|} + \frac{1}{2}\mathbf{1}_M$ with $\mathbf{x} \in \mathbb{R}^M$.

C. Update $(\boldsymbol{\eta}_1^{t+1}, \boldsymbol{\eta}_2^{t+1}, \eta_3^{t+1})$

The dual variables are updated by the conventional gradient ascent method as

$$\boldsymbol{\eta}_1^{t+1} = \boldsymbol{\eta}_1^t + \rho_1(\mathbf{z}^{t+1} - \mathbf{z}_1^{t+1}), \tag{32}$$

$$\boldsymbol{\eta}_2^{t+1} = \boldsymbol{\eta}_2^t + \rho_1(\mathbf{z}^{t+1} - \mathbf{z}_2^{t+1}), \tag{33}$$

$$\eta_3^{t+1} = \eta_3^t + \rho_3(\mathbf{1}_M^T\mathbf{z} - M_0). \tag{34}$$

Although the problem in (24) is non-convex, ADMM can still provide a guarantee of convergence to a Karush–Kuhn–Tucker point [20] by updating the above parameters.

V. Simulation and Discussion

In this section, we present numerical examples to demonstrate the effectiveness of the optimal mixed-precision arrangement. We consider three array structures, i.e., ULA, nested array and co-prime array, assuming the total antenna element $M = 30$ and the number of high-precision ADCs $M_0 = 8$. We consider four situations for the mixed-ADC based architecture:

1) $\{\delta_i = 1\}_{i=1}^{8}$ and $\{\delta_i = 0\}_{i=9}^{30}$;
2) $\{\delta_i = 0\}_{i=1}^{22}$ and $\{\delta_i = 1\}_{i=23}^{30}$;
3) $\{\delta_i = 0\}_{i=1}^{10}$, $\{\delta_i = 1\}_{i=11}^{18}$ and $\{\delta_i = 0\}_{i=19}^{30}$;
4) The optimal mixed-precision arrangement computed by the ADMM.

It is assumed that three independent targets locate at $\{\theta_1 = 10°, \theta_2 = 15°, \theta_3 = 30°\}$. All sources have an equal power, and the SNR is defined as SNR $= p/\sigma^2$. For the one-bit ADC system and mixed-ADC based architecture, the time-vary threshold has the real and imaginary parts selected randomly and equally likely from a predefined eight-element set $\{-h_{\max}, -h_{\max} + \Delta, \ldots, h_{\max} - \Delta, h_{\max}\}$ with $h_{\max} = \sqrt{p_{\text{out}}}$ and $\Delta = \frac{h_{\max}}{7}$, where $\sqrt{p_{\text{out}}}$ is the average received signal power at the I/Q channels. In our simulation, we set the initial solution $\mathbf{z}^0 = \mathbf{1}_M$, $\rho_1 = \rho_2 = \rho_3 = 1.6$, and the matrix $\mathbf{D}$ is normalized.

In Fig. 1, the iterative procedure of the ADMM using ULA is illustrated. After only 10 iteration, the initialized value approaches an almost binary state, on which the CRB is close to the global maximum. And the result is consistent with [18], that the high-precision ADCs are placed evenly around the edge of the ULA as expected.

Fig. 2 and Fig. 3 plot the CRBs versus SNR for θ_1 (degress) on different mixed-ADC architecture using nested array and co-prime array, respectively, where situations 1, 2, 3 and 4 are denoted as "Mixed-ADC1", "Mixed-ADC2", "Mixed-ADC3" and "Mixed-ADC4", respectively. The optimal mixed-precision arrangement is distinct for arrays with different structure, with the exception that high-precision ADCs are arranged at the edge of the array, which can be explained by the fact that the optimal mixed-precision arrangement has the largest antenna spacing for high-precision ADCs. Compared with the pure one-bit system, mixed-ADC architecture can significantly improve the performance. As SNR increases, the performance gap between the optimal mixed-precision arrangement and others widens. Notably, the CRB of DOA

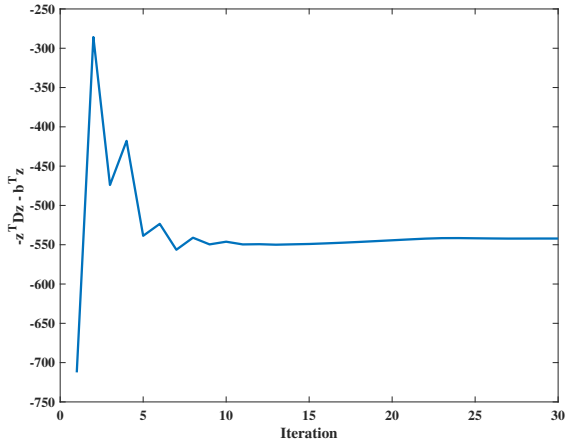

(a) objective value versus iteration

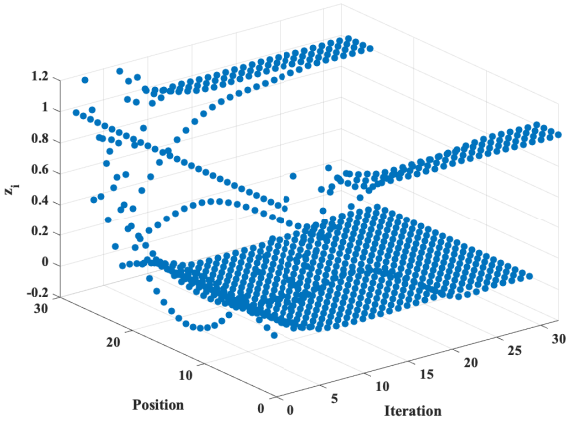

(b) solution changes versus iteration

Fig. 1. The optimization procedure of ADMM using ULA.

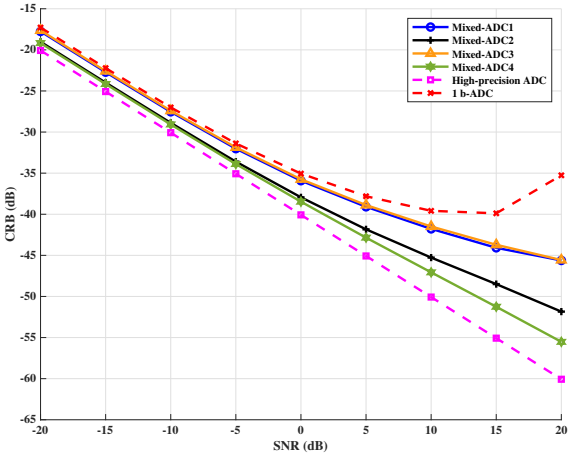

Fig. 2. CRB versus SNR on different mixed-ADC architecture using nested array with $N_1 = N_2 = 15$. The optimal mixed-precision arrangement is obtained as $\{\delta_i = 1\}_{i=1}^{2}$, $\{\delta_i = 0\}_{i=4}^{25}$ and $\{\delta_i = 1\}_{i=25}^{30}$.

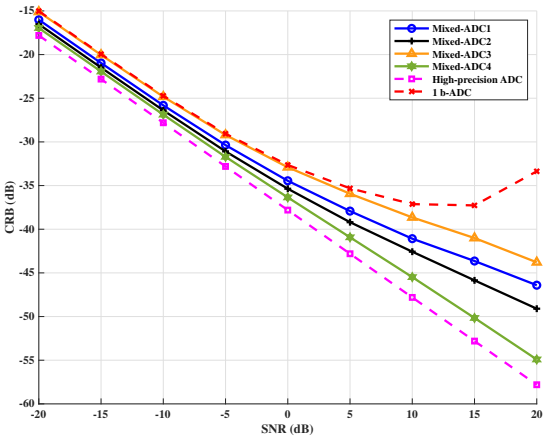

Fig. 3. CRB versus SNR on different mixed-ADC architecture using co-prime array with $N_1 = 11, N_2 = 10$. The optimal mixed-precision arrangement is obtained as $\{\delta_i = 1\}_{i=1}^{3}$, $\{\delta_i = 0\}_{i=4}^{25}$ and $\{\delta_i = 1\}_{i=26}^{30}$.

on the optimal mixed-precision arrangement is almost 10 dB lower than others when SNR $= 20$ dB. Therefore, a random mixed-precision arrangement is inappropriate as it could result in significant performance losses.

VI. Conclusion

In this work, we explore the arrangement of one-bit and high-precision ADCs in SLAs with arbitrary structure under a mixed-ADC based architecture. We analyze the CRB on different mixed-precision arrangement when the fixed number of ADCs is given. We simplified the problem into a 0-1 integer quadratic programming and solve it efficiently using the ADMM algorithm to obtain the optimal mixed-precision arrangement. Numerical examples show that SLAs, such as nested array and co-prime array, can achieve a lower CRB by using optimal mixed-precision arrangement, especially in a large SNR scene.

References

[1] E. Tuncer and B. Friedlander, *Classical and modern direction-of-arrival estimation*, Academic Press, 2009.

[2] S. Sun, A. P. Petropulu, and H. V. Poor, "MIMO radar for advanced driver-assistance systems and autonomous driving: Advantages and challenges," *IEEE Signal Process. Mag.*, vol. 37, no. 4, pp. 98–117, 2020.

[3] H. Krim and M. Viberg, "Two decades of array signal processing research: The parametric approach," *IEEE Signal Process. Mag.*, vol. 13, no. 4, pp. 67–94, 1996.

[4] S. Haykin, J. Litva, and T. J. Shepherd, *Radar array processing*, Springer, 1993.

[5] P. Stoica and A. Nehorai, "Performance study of conditional and unconditional direction-of-arrival estimation," *IEEE Trans. Acoust., Speech, and Signal Process.*, vol. 38, no. 10, pp. 1783–1795, 1990.

[6] A. Moffet, "Minimum-redundancy linear arrays," *IEEE Trans. Antennas Propag.*, vol. 16, no. 2, pp. 172–175, 1968.

[7] P. P. Vaidyanathan and P. Pal, "Sparse sensing with co-prime samplers and arrays," *IEEE Trans. Signal Process.*, vol. 59, no. 2, pp. 573–586, 2010.

[8] P. Pal and P. P. Vaidyanathan, "Nested arrays: A novel approach to array processing with enhanced degrees of freedom," *IEEE Trans. Signal Process.*, vol. 58, no. 8, pp. 4167–4181, 2010.

[9] R. H. Walden, "Analog-to-digital converter survey and analysis," *IEEE J. Sel. Areas Commun.*, vol. 17, no. 4, pp. 539–550, 1999.

[10] O. Bar-Shalom and A. J. Weiss, "DOA estimation using one-bit quantized measurements," *IEEE Trans. Aerosp. Electron. Syst.*, vol. 38, no. 3, pp. 868–884, 2002.

[11] S. Sedighi, M. Soltanalian, and B. Ottersten, "On the performance of one-bit DOA estimation via sparse linear arrays," *IEEE Trans. Signal Process.*, vol. 69, pp. 6165–6182, 2021.

[12] C. Liu and P. P. Vaidyanathan, "One-bit sparse array doa estimation," in *Proc. IEEE Int. Conf. Acoust., Speech Signal Process.*, New Orleans, USA, Mar. 2017, pp. 3126–3130.

[13] M. S. Stein, S. Bar, J. A. Nossek, and J. Tabrikian, "Performance analysis for channel estimation with 1-bit ADC and unknown quantization threshold," *IEEE Trans. Signal Process.*, vol. 66, no. 10, pp. 2557–2571, 2018.

[14] J. Mo and R. W. Heath, "High SNR capacity of millimeter wave MIMO systems with one-bit quantization," in *Proc. Inf. Theory Appl. Workshop*, San Diego, CA, USA, Feb. 2014, pp. 1–5.

[15] N. Liang and W. Zhang, "Mixed-ADC massive MIMO," *IEEE J. Sel. Areas Commun.*, vol. 34, no. 4, pp. 983–997, 2016.

[16] B. Shi, L. Zhu, W. Cai, N. Chen, T. Shen, P. Zhu, F. Shu, and J. Wang, "On performance loss of DOA measurement using massive MIMO receiver with mixed-ADCs," *IEEE Wireless Commun. Lett.*, 2022.

[17] Y. Cheng, X. Shang, and F. Liu, "CRB analysis for mixed-ADC PMCW MIMO Radar," in *Proc. CIE Int. Conf. Radar*, Hai Kou, China, Dec. 2021, pp. 1032–1037.

[18] X. Zhang, Y. Cheng, X. Shang, and J. Liu, "Optimal mixed-ADC arrangement for DOA estimation via CRB using ULA," in *Proc. IEEE Int. Conf. Acoust., Speech Signal Process.*, Rhodes Island, Greece, Jun. 2023.

[19] C. Li, R. Zhang, J. Li, and P. Stoica, "Bayesian information criterion for signed measurements with application to sinusoidal signals," *IEEE Signal Process. Lett.*, vol. 25, no. 8, pp. 1251–1255, 2018.

[20] B. Wu and B. Ghanem, "ℓ_p-box ADMM: A versatile framework for integer programming," *IEEE Trans. Pattern Anal. Mach. Intell.*, vol. 41, no. 7, pp. 1695–1708, 2018.